International Journal of Industrial Engineering & Production Research March 2025, Vol. 36, No. 1: 171-180
DOI: 10.22068/ijiepr.36.1.2223

RESEARCH PAPER

Young's Modulus Optimisation of Triply Periodic Minimal Surfaces using Full Factorial Design

Nor Hasrul Akhmal Ngadiman[1,*], Nur Syahirah Mustafa[2], Izman Sudin[3], Denni Kurniawan[4]

Received 18 November 2024; Revised 10 January 2025; Accepted 05 February 2025;

ABSTRACT
Bone tissue scaffolds that closely mimic the mechanical and biological properties of natural bone is critical for enhancing the outcomes in treatment of bone tissue damages. This study introduces an optimisation approach to designing bone tissue engineering scaffolds using Triply Periodic Minimal Surface (TPMS) structures, evaluated through a Full Factorial Design methodology. Finite Element Analysis was applied to simulate the TPMS scaffolds under mechanical loading. The influence of key factors of strut thickness, unit cell configuration, and TPMS type, on the scaffold's mechanical performance, specifically targeting Young's modulus was evaluated. By employing Full Factorial Design, this study generates empirical models of Young's modulus as a function of those key factors. Primitive and Gyroid TPMS structures emerged as optimal, achieving Young's modulus values of 4912.3 MPa and 4666.7 MPa, respectively, with configurations of 0.01 mm strut thickness in a 3-unit cell construct. These results demonstrate that optimised TPMS scaffolds can meet the mechanical demands of bone tissue while providing adequate porosity for cell proliferation and nutrient transport, essential for effective bone regeneration.

KEYWORDS: *Bone tissue engineering; Scaffold; Young's modulus; Triply periodic minimal surface; Full factorial design; Optimization.*

1. Introduction

The human skeletal system is vital for providing structural support, safeguarding organs, facilitating mobility, storing minerals, and producing blood cells [1]. Despite their durability, bones are susceptible to a range of traumas and disorders [2]. To fix these bone damages, tissue engineering which creates viable tissues from the patient's own cells is being researched. Bone tissue engineering holds the potential to address the issues of present clinical treatments [3-5].
Scaffold is a key component of bone tissue engineering where a biomaterial with porous three-dimensional structure provides support for cell attachment and growth, mimicking extra-cellular matrix [6]. The strength and porosity of the scaffold should be designed to be similar to the original bone. This challenge can be addressed by designing suitable structure with a high surface area to volume ratio [7, 8] and adequate porosity to facilitate the nutrients transport and cell growth. At the same time, the structure should not compromise the scaffold's mechanical strength. The development of additive manufacturing makes it possible to create intricate structure of bone tissue engineering scaffolds [9].
Structures of bone tissue engineering scaffolds include Voronoi Tessellation, Functionally Graded Scaffold, and Triply Periodic Minimal Surface (TPMS) [10]. Among these, TPMS is of interest in this study for combining high surface area to volume ratio, porosity, and mechanical strength [11]. The curved configurations of TPMS offer enhanced
cell proliferation and tissue integration compared to conventional lattice structures [12, 13]. TPMS structure can be categorized into stretching surface and bending surface TPMS based on their deformation mechanisms [14]. Although there are various TPMS structures that are available through the parametric equation such as Gyroid [15], Schwarz P (Primitive) [16], Schwarz D (Diamond) [17], Lidinoid [17], Neovius [18], I-WP [10], Fisher-Koch S [19], and Fisher-Koch Y [20], this study only considers few options from the TPMS categories due to their ability to match the host tissue and avoiding stress shielding [21]. The structures are Gyroid, Primitive, Diamond and Lidinoid. As mentioned previously, according

* *Corresponding author: Nor Hasrul Akhmal Ngadiman*
norhasrul@utm.my

1. *Faculty of Mechanical Engineering, Universiti Teknologi Malaysia, 81310 Skudai, Johor, Malaysia*
2. *Faculty of Mechanical Engineering, Universiti Teknologi Malaysia (UTM), 81310 Skudai, Malaysia*
3. *Faculty of Mechanical Engineering, Universiti Teknologi Malaysia, 81310 Skudai, Malaysia*
4. *Mechanical Engineering Programme Area, Universiti Teknologi Brunei, Gadong BE1410, Brunei*

to their deformation mechanisms, Gyroid and Diamond belong to the bending surface category, meanwhile Primitive and Lidinoid are the examples of stretching surface TPMS. Using polymeric biomaterials, TPMS scaffolds can attain Young's modulus up to 2670 MPa, enabling their use for cartilage and cancellous bone [22]. A study on Diamond and Gyroid TPMS structures with a porosity of 50% resulted in Young's modulus values of 7700 MPa and 4800 MPa, respectively [23]. Other studies reported that TPMS possesses significant amount of Young's Modulus due to its unique structure that enables it to maintain less stress concentration points [22, 24]. When designing TPMS structure for bone tissue engineering scaffolds, several parameters must be considered to enable the development of scaffolds that will fulfil the demand of having high mechanical properties without reducing the ability of the scaffold to facilitate the cell viability and cell growth during the recovery process. Thickness of the strut should be considered because it affects the pore size. For successful bone tissue repair, the scaffold should have a pore diameter ranging from 300 μm to 900 μ [25]. Another parameter which affects the pore size is the strut diameter. This study aims to identify the optimal TPMS structure design with regards to the scaffold's Young's modulus. A finite element analysis was conducted by developing the modelled TPMS designs, running the simulation by applying load and boundary conditions, and extracting the Young's modulus from the simulation. Statistical analysis using full factorial design was used in determining the optimum TPMS design. Despite its drawback which requires complete set of parameters combination, full factorial design was selected in this study for its ability to determine the effect of each parameter. Regarding the finite element modelling, simulation is usually done for a portion of the entire construct. Scaffolds that have unit cells, like ones with conventional lattice and TPMS structures, were often modelled in limited number of unit cells only to save computational resources. Some researchers simulated the scaffold in only 3x3x3 unit cells [26, 27] while other in 5x5x5 unit cells [28]. Considering the number of unit cells influences the resulting Young's modulus of the scaffolds, this study also considers it as a parameter.

Having mentioned all of the significant parameters that could affect the performance of the scaffold, it is important to note that there is still a gap to define a suitable scaffold design that will not only able to maintain an excellent mechanical strength (Young's modulus) while aiding to expedite the bone regeneration process.

2. Materials and Methods

2.1. Design of triply periodic minimal surface structures

Four TPMS designs were selected, namely Gyroid, Primitive, Diamond, and Lidinoid. The TPMS scaffolds were modelled using Minisurf [29] which operates on the Matlab Runtime, a freely available Matlab compiler. Finite element analysis on the TPMS scaffolds was using commercially available software, Abaqus (Dassault Systèmes, France).

The TPMS design was imported from MiniSurf into Abaqus and the model's characteristics were assigned. The biomaterial used was polylactic acid (PLA) within its elastic region with 3000 MPa Young's modulus and 0.3 Poisson's ratio. PLA was chosen in this study since it is known to be non-toxic, and most importantly, it is approved by FDA [30]. After assigning the material properties, a load and boundary condition were applied (Figure 1). The structure was displaced on top with a compression of 5% of its height. The displacement lasted for 1 second, with increments of 0.01 seconds. The bottom surface of the structure had a fixed boundary condition.

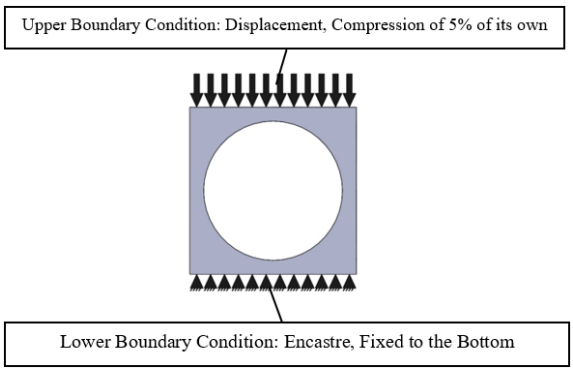

Fig.1. Boundary condition of the structure

A mesh convergence test was conducted by repeatedly simulating the structure using multiple mesh sizes, ranging from 0.01 mm to 0.1 mm. This was done to verify that the mesh is capable of adequately supporting the structure and providing an appropriate response to the assigned boundary conditions. The mesh

convergence test indicated that the optimal global seedings should be set to 0.05 mm. Tetrahedral element was selected as the element type as it can be fitted into any simulation domain shape, and it is recognized as the most commercial meshes in most software [31].

2.2. Preliminary analysis

To reduce the number of runs in full factorial design, a preliminary analysis was conducted. This is intended to narrow down the number of designs for further analysis from four to two. The design and porosity of the four TPMS structures are stated in Table 1.

2.3. Optimisation of TPMS designs using full factorial design

The factors and levels of the TPMS designs were determined from results by previous researchers [25, 28]. The levels were scaled into three levels which are low (-1), centre point (0) and high (+1) as shown in Table 2. These levels were set as the upper and lower limit for the statistical analysis. Commercially available statistical software Design Expert (Stat-Ease, USA) was used for this purpose. A Full Factorial experimental design which is a type of Design of Experiment (DoE) method was used in this study to determine the optimum factors that would result in the best response. A factorial design is a reliable tool to evaluate the effect of parameters on the variable [32]. A three-level reaction was used with one categorical factor resulting a total of 12 runs (Table 3). The TPMS structure factor only considered two of the best, as determined by the preliminary analysis.
The simulation for the optimisation process was conducted using the same procedure as the preliminary analysis to estimate the Young's Modulus of a single-unit cell TPMS. The TPMS structures were refined by adjusting the thickness of the struts and the number of unit cells. These adjustments were made based on the combinations specified in the experimental matrix design. The results acquired from the simulation were gathered and examined utilising the stress-strain graphs. The slope of the graph, representing Young's Modulus, was subsequently inputted into the experimental matrix design.

Tab.1. Design and porosity value of the structures

Model	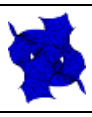		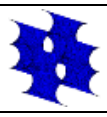	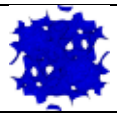
Model name	Gyroid	Primitive	Diamond	Lidinoid
Structure volume (mm^3)	1	1	1	1
Porosity (%)	94.60	95.89	93.31	89.22

Tab.2. Significant factors and their levels

Factor	**Type of Factor**	**Low level**	**Centre point**	**High level**
TPMS Structure	Categorical	TPMS Structure 1	-	TPMS Structure 2
Strut Thickness (mm)	Numerical	0.01	0.035	0.06
Number of Unit Cells	Numerical	3	4	5

Tab.3. Experimental matrix data (2 full factorial design)

Run	**Block**	**Factor A: TPMS Structure**	**Factor B: Strut Thickness (mm)**	**Factor C: Number of Unit Cells**
1	Block 1	TPMS Structure 1	0.01	3
2	Block 1	TPMS Structure 2	0.01	3
3	Block 1	TPMS Structure 1	0.06	3
4	Block 1	TPMS Structure 2	0.06	3
5	Block 1	TPMS Structure 1	0.01	5
6	Block 1	TPMS Structure 2	0.01	5
7	Block 1	TPMS Structure 1	0.06	5
8	Block 1	TPMS Structure 2	0.06	5
9	Block 1	TPMS Structure 1	0.035	4
10	Block 1	TPMS Structure 2	0.035	4
11	Block 1	TPMS Structure 1	0.035	4
12	Block 1	TPMS Structure 2	0.035	4

The data was statistically analysed for numerical optimisation using Analysis of Variance (ANOVA) in the statistical software. The experiments' significance was established, and an equation was generated by statistical analysis [33] As a main requirement, the porosity of the construct should exceed 80%.

To verify the accuracy of the optimisation results, a confirmation run was conducted. The confirmation run includes the adjusted parameters as well as the estimated Young's Modulus using a mathematical equation. The confirmation run is expected to exhibit an error of less than 5%. The following equation was used to calculate the percentage of error.

$$\text{Percentage of Error} = \frac{\text{Predicted Value} - \text{Actual Value}}{\text{Actual Value}} \times 100\% \quad \text{(Eq.1)}$$

3. Result and Discussion

3.1. Preliminary analysis result

The Young's Modulus of the four TPMS designs was determined from a preliminary investigation. The location of the assessed element for analysing the stress and strain curve data was selected to be the point with the highest von Mises stress, as indicated in Figure 2 and compiled in Table 4.

Tab.4. Young's modulus and porosity of TPMS structure

Unit Cell Structure	Young's Modulus (MPa)	Porosity (%)
Primitive	5157.10	95.89
Gyroid	3981.20	94.60
Diamond	3803.70	93.31
Lidinoid	3530.60	89.22

3.2. Optimisation of TPMS designs using full factorial design

Table 5 shows the results obtained from finite element analysis of twelve runs in Full Factorial Design which include three factors of TPMS structure, strut thickness, and number of unit cells. The highest Young's modulus of 4.91 GPa resulted from combination of Primitive design at the lowest thickness where the model only used 3x3x3 unit cells.

Analysis of Variance was employed to assess the significance of the factors on the Young's modulus of the scaffold (Table 6). In addition to each main factor, the ANOVA also calculated the effect of interaction between two and all three main factors. The Model's F-value of 23.87 shows that it is significant. Using "Prob >F" set to be less than 0.05 for the factors to be significant.

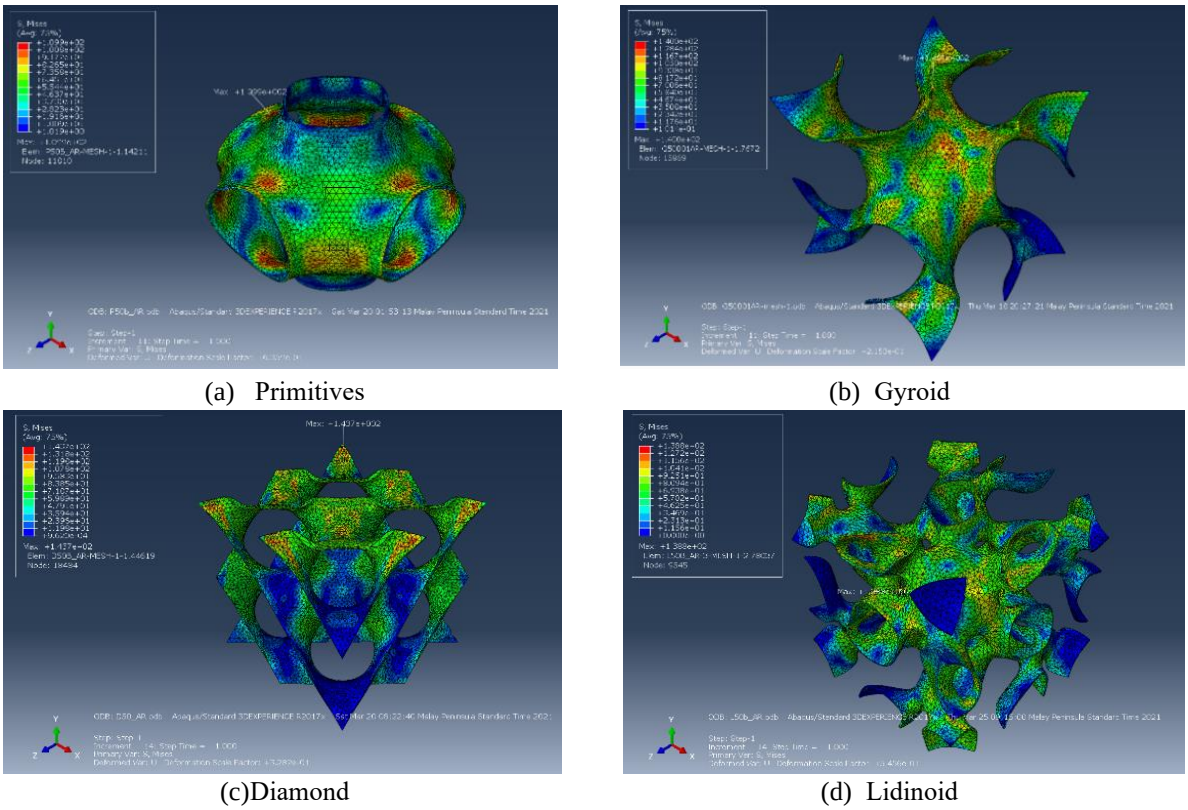

(a) Primitives (b) Gyroid

(c)Diamond (d) Lidinoid

Fig.2. Stress-strain analysis of preliminary study of TPMS

Tab.5. Data for Young's modulus in full factorial design

Run	Block	Factor A TPMS Structure	Factor B Strut Thickness (mm)	Factor C Number of Unit Cells	Young's Modulus (MPa)
1	Block 1	Primitive	0.01	3	4912.3
2	Block 1	Gyroid	0.01	3	4666.7
3	Block 1	Primitive	0.06	3	4280.7
4	Block 1	Gyroid	0.06	3	4066.7
5	Block 1	Primitive	0.01	5	3549.4
6	Block 1	Gyroid	0.01	5	3371.9
7	Block 1	Primitive	0.06	5	3218.7
8	Block 1	Gyroid	0.06	5	3057.8
9	Block 1	Primitive	0.035	4	4235.6
10	Block 1	Gyroid	0.035	4	3846.3
11	Block 1	Primitive	0.035	4	4023.82
12	Block 1	Gyroid	0.035	4	3653.99

Tab.6. ANOVA for Young's modulus

Source	Sum of Squares	DF	Mean Square	F Value	Prob >F	
Model	3482319	7	497474	23.87	0.01	significant
A	202055.8	1	202056	9.70	0.05	
B	440109.6	1	440110	21.11	0.02	
C	2794957	1	2794957	134.08	0.00	
AB	290.405	1	290	0.01	0.91	
AC	1836.18	1	1836	0.09	0.79	
BC	43041.78	1	43042	2.06	0.25	
ABC	28.125	1	28	0.00	0.97	
Curvature	6507.956	1	6508	0.31	0.62	not significant
Residual	62534.12	3	20845			
Lack of Fit	21616.2	1	21616	1.06	0.41	not significant
Pure Error	40917.91	2	20459			
Cor Total	3551361	11				

Std. Dev.	144	**R-Squared**	0.98
Mean	3907	**Adj R-Squared**	0.94
C.V. %	3.70	**Pred R-Squared**	-0.20
PRESS	4.275E+006	**Adeq Precision**	15.31

From ANOVA analysis, it can be seen that the model is significant. This indicates that the Factors B and C which correspond to strut thickness and number of unit cells, respectively, are significant. The Model's equation's R-Squared and Adjusted R-Squared of 0.9824 and 0.9412, respectively, are high and reasonable, further indicates significance. The mathematical equation for this model is shown in Eq. 2 for Primitive and Eq. 3 for Gyroid.

$$\text{Young's Modulus (Primitives)} = 7203.25125 - 21659.00B - 711.54C \quad \text{(Eq.2)}$$

$$\text{Young's Modulus (Gyroid)} = 6784.65875 - 20577.00B - 675.99C \quad \text{(Eq.3)}$$

Since the curvature is not significant in the model, there is no need to further investigate the structure by using second order model. To verify the model's adequacy, the normal probability plots of residuals and the plots of residuals versus the predicted response are shown in the Figures 3 and 4, respectively. The normal plot is used to recognise any outliers or factors that can contribute to noise or disturbance in optimisation. In this study, the normal plot is normally distributed with no outliers, rendering it accurate and reliable for optimisation. From Figure 4, the data were scattered randomly no unusual structure is apparent and, hence, the model can be used further.

To ultimately confirm the adequacy of the model, confirmation runs were conducted on some of the factors' combinations (Table 7). It was identified that the calculated Young's modulus was very similar to the simulated Young's modulus, with error of less than 1%.

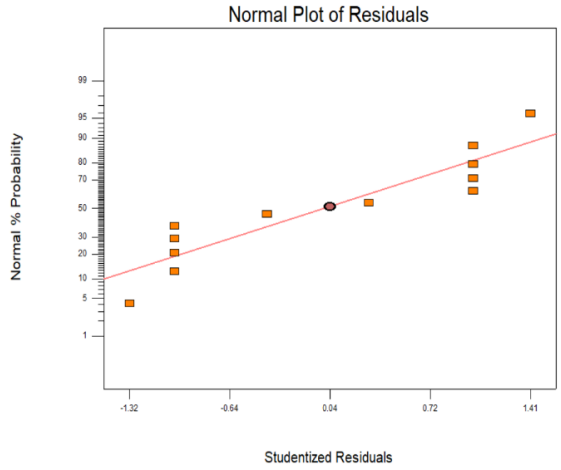

Fig.3. Normal plot for Young's modulus

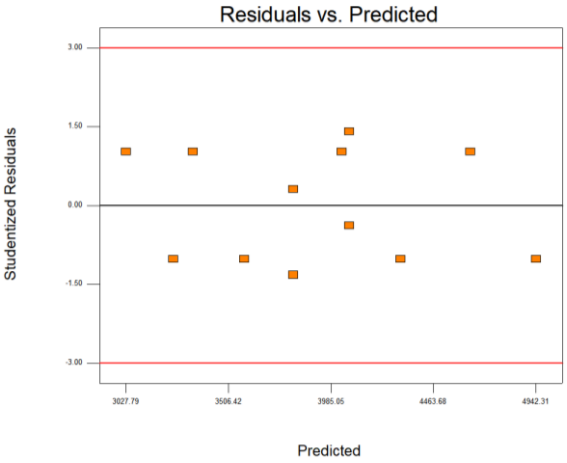

Fig.4. Residuals vs. predicted plot for young's modulus

This study found that the Young's modulus of the scaffolds is inversely proportional to the strut thickness. This finding agrees with previous studies [34, 35]. This counterintuitive phenomenon can be attributed to higher bending moments experienced by thicker struts, leading to increased deflection. Also, as strut thickness increases, localised stress concentrations occur, due to diminishing ability of the scaffold to distribute loads effectively. It should be noted that previous study advised to set the minimum strut thickness [30] where possible to avoid the possibility of self-intersection problems [36].

TPMS structures demonstrate an inverse correlation between the number of unit cells and the resulting Young's Modulus as illustrated in this study. This can be explained by the fact that with more unit cells, loads are distributed over a larger area and across more struts. This distribution can lead to a reduction in local stiffness, as each individual strut bears less load compared to a scenario with fewer unit cells where each strut may be required to support more forces. Also, as the number of unit cells increases, the connectivity between struts may become more complex. This increased connectivity can introduce more points of flexibility within the structure, leading to an overall decrease in stiffness.

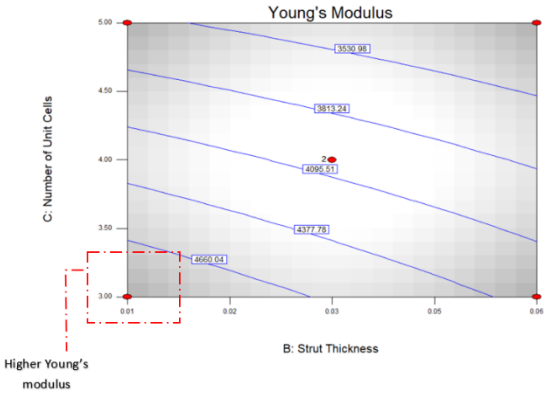

Fig.5. Contour plot for Young's modulus for Primitive

It is recognized that Primitive design results in higher Young's modulus compared to Gyroid. Primitive shows 5.2% higher Young's modulus while having 1.4% higher porosity compared to Gyroid. This can be attributed to the alignment of struts of the TPMS designs. Primitive's alignment of struts is typically more uniform and direct, allowing loads to be carried efficiently along the struts, resulting in a higher effective Young's modulus as the material can better resist deformation.

Tab.7. Confirmation run of optimized TPMS design criteria

Types of TPMS	Strut Thickness (mm)	No. of Unit Cell	Calculated Young's Modulus (MPa)	Simulated Young's Modulus (MPa)	Error (%)
Primitives	0.01	3	4935.65	4912.30	0.48
	0.02	4	4164.63	4128.97	0.86
	0.06	5	3248.71	3218.70	0.92
Gyroid	0.02	3	4636.69	4666.70	0.64
	0.01	5	3341.89	3371.90	0.90
	0.06	5	3027.79	3057.80	0.99

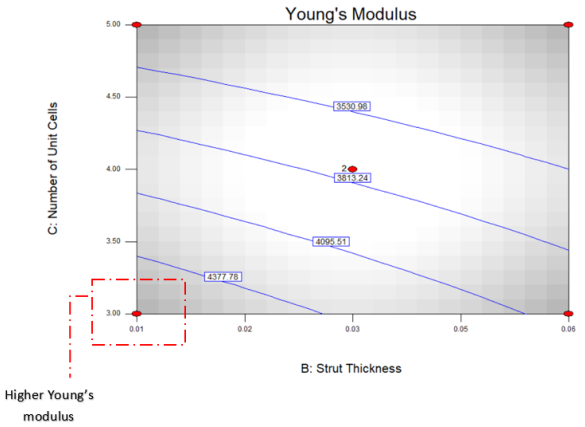

Fig.6. Contour plot for Young's modulus for Gyroid

Gyroid's curvature can introduce bending moments that affect how forces are transmitted through the structure. This bending can lead to localised stress concentrations and a reduction in stiffness compared to the more straightforward load paths in Primitive.

Lastly, it can be agreed that Primitive is still superior as compared to any other TPMS structures in terms of porosity and Young's modulus. It can be proven that Primitive is still dominant during the one-unit cell structure, and in the optimization stage, it is found out that Primitive is a still more reliable design in producing a higher Young's modulus structure as compared to Gyroid. Hence, it is obvious that Primitive should be chosen as the most superior TPMS structure, thus it can be used as the foundation for the upcoming researches.

4. Conclusion

This study presents the application of Full Factorial Design in optimising the parameters for Triply Periodic Minimal Surface scaffolds tailored for bone tissue engineering. By systematically analysing the effects of key factors of strut thickness, unit cell configuration, and TPMS type through a Full Factorial Design approach, this study is able to identify configurations that maximise Young's modulus while maintaining essential porosity. The Primitives and Gyroid structures, optimised through this methodology, exhibited Young's modulus values of 4912.3 MPa and 4666.7 MPa, respectively, using strut thicknesses of 0.01 mm for models with a 3-unit cell configuration. This study underscores the capability of these TPMS structures to support cartilage and cancellous bones while having >94% porosity when used as bone tissue engineering scaffolds.

The use of Full Factorial Design allowed for an exploration of interactions among factors, in addition to the main factors. With the help of Analysis of Variance to determine the significance of the model and its factors, this statistical method can be used to quantify the effect of factors to the measured result. Although the validity of the resulting mathematical models is limited to the levels of the factors, this work establishes a ground to where the future research builds upon. Since TPMS can be considered as a complex geometry, it can establish a foundation to enable more researches that is not limited to only bone tissue engineering, but it will create a more innovative products that will utilise the integration between engineering design, optimization and 3D printing in various field.

Further studies should explore more capabilities of the TPMS structure that can be employed as the design of the scaffold. It is suggested that the future research to be able to investigate the biodegradation rate of the TPMS scaffold since it is important for the scaffold to withstand the pressure as much as the host tissue during the recovery process. In addition, an in-vitro study on the effect of the TPMS-based scaffolds should be conducted in order to be adopted in real-life clinical used. It is crucial that the TPMS scaffold to be capable of facilitating bone healing process in an environment that can mimic the actual surroundings of the damaged bones.

Acknowledgement

The authors would like to acknowledge the financial support from Ministry of Higher Education Malaysia under Fundamental Research Grant Scheme (FRGS) (FRGS/1/2024/TK10/UTM/02/8) (R.J130000.7824.5F739) and Universiti Teknologi Malaysia for the grant funding (Q.J130000.3024.04M90).

Conflicts of Interest

The authors declare no conflicts of interest.

References

[1]. A. Wawrzyniak and K. Balawender, "Structural and metabolic changes in bone", Animals, vol. 12, no. 15, 2022, p. 1946.

[2]. E. Marin, "Forged to heal: The role of metallic cellular solids in bone tissue engineering", Materials Today Bio, vol. 23, 2023, p. 100777.

[3]. N. Arifin, I. Sudin, N. H. A. Ngadiman, and M. S. A. Ishak, "A comprehensive review of biopolymer fabrication in additive manufacturing processing for 3D-tissue-engineering scaffolds," Polymers, vol. 14, no. 10, 2022, p. 2119.

[4]. E. Fallahiarezoudar, N. H. A. Ngadiman, N. M. Yusof, A. Idris, and M. S. A. Ishak, "Development of 3D Thermoplastic Polyurethane (TPU)/Maghemite (Υ-Fe_2O_3) Using Ultra-Hard and Tough (UHT) Bio-Resin for Soft Tissue Engineering", Polymers, vol. 14, no. 13, 2022, p. 2561.

[5]. M. Schlund, A. Depeyre, S. K. Ranganath, P. Marchandise, J. Ferri, and F. Chai, "Rabbit calvarial and mandibular critical-sized bone defects as an experimental model for the evaluation of craniofacial bone tissue regeneration", Journal of Stomatology, Oral and Maxillofacial Surgery, vol. 123, no. 6, 2022, pp. 601-609.

[6]. N. H. A. Ngadiman, N. M. Yusof, A. Idris, E. Fallahiarezoudar, and D. Kurniawan, "Novel processing technique to produce three dimensional polyvinyl alcohol/ maghemite nanofiber scaffold suitable for hard tissues", Polymers, vol. 10, no. 4, 2018, p. 353.

[7]. N. H. A. Ngadiman, N. M. Yusof, A. Idris, E. Misran, and D. Kurniawan, "Development of highly porous biodegradable γ-Fe_2O_3/ polyvinyl alcohol nanofiber mats using electrospinning process for biomedical application", Materials Science and Engineering: C, vol. 70, 2017, pp. 520-534.

[8]. Y. Zhang, M. Zhang, D. Cheng, S. Xu, C. Du, L. Xie, and W. Zhao, "Applications of electrospun scaffolds with enlarged pores in tissue engineering", Biomaterials Science, vol. 10, no. 6, 2022, pp. 1423-1447.

[9]. T. Tom, S. P. Sreenilayam, D. Brabazon, J. P. Jose, B. Joseph, K. Madanan, and S. Thomas, "Additive manufacturing in the biomedical field-recent research developments", Results in Engineering, vol. 16, 2022, p. 100661.

[10]. X. Wang, T. Gao, C. Shi, Y. Zhou, Z. Li, and Z. Wang, "Effect of geometric configuration on compression behavior of 3D-printed polymeric triply periodic minimal surface sheets", Mechanics of Advanced Materials and Structures, vol. 30, no. 11, 2023, pp. 2304-2314.

[11]. R. Pugliese and S. Graziosi, "Biomimetic scaffolds using triply periodic minimal surface-based porous structures for biomedical applications", SLAS technology, vol. 28, no. 3, 2023, pp. 165-182.

[12]. N. S. Mustafa, N. H. Akhmal, S. Izman, M. H. Ab Talib, A. I. M. Shaiful, M. N. B. Omar, N. Z. Yahaya, and S. Illias, "Application of computational method in designing a unit cell of bone tissue engineering scaffold: A review", Polymers, vol. 13, no. 10, 2021, p. 1584.

[13]. N. H. A. Ngadiman, N. S. Mustafa, A. A. Omar Alkaff, and M. Z. Mat Saman, "Quality improvement on mechanical properties of FDM 3D printed triply periodic minimal surfaces (TPMS) structure for tissue engineering scaffold", Journal of Mechanical Engineering (JMechE), vol. 13, no. 1, 2024, pp. 31-54.

[14]. S. Liu, J. Chen, T. Chen, and Y. Zeng, "Fabrication of trabecular-like beta-tricalcium phosphate biomimetic scaffolds for bone tissue engineering", Ceramics International, vol. 47, no. 9, 2021, pp. 13187-13198.

[15]. N. Wang, G. K. Meenashisundaram, S. Chang, J. Y. H. Fuh, S. T. Dheen, and A. S. Kumar, "A comparative investigation on the mechanical properties and cytotoxicity of Cubic, Octet, and TPMS gyroid structures fabricated by selective laser melting of stainless steel 316L", Journal of the Mechanical Behavior of Biomedical Materials, vol. 129, 2022, p. 105151.

[16]. X. Guo, J. Ding, X. Li, S. Qu, X. Song, J. Y. H. Fuh, W. F. Lu, and W. Zhai, "Enhancement in the mechanical behaviour of a Schwarz Primitive periodic minimal surface lattice structure design", International Journal of Mechanical Sciences, vol. 216, 2022, p. 106977.

[17]. T. Röver, M. Kuehne, F. Bischop, L. Clague, B. Bossen, and C. Emmelmann, "Design and numerical assessment of an additively manufactured Schwarz diamond triply periodic minimal surface fluid-fluid heat exchanger", Journal of laser

applications, vol. 35, no. 4, 2023.

[18]. G. J. Shah, A. Nazir, S.-C. Lin, and J.-Y. Jeng, "Design for additive manufacturing and investigation of surface-based lattice structures for buckling properties using experimental and finite element methods", Materials, vol. 15, no. 11, 2022, p. 4037.

[19]. V. Baumer, E. Gunn, V. Riegle, C. Bailey, C. Shonkwiler, and D. Prawel, "Robocasting of Ceramic Fischer–Koch S Scaffolds for Bone Tissue Engineering", Journal of functional biomaterials, vol. 14, no. 5, 2023, p. 251.

[20]. Z.-y. Zhang, H. Zhang, J. Zhang, S.-k. Qin, and M.-d. Duan, "Study on flow field characteristics of TPMS porous materials", Journal of the Brazilian Society of Mechanical Sciences and Engineering, vol. 45, no. 4, 2023, p. 188.

[21]. J. Jiang, Y. Huo, X. Peng, C. Wu, H. Zhu, and Y. Lyu, "Design of novel triply periodic minimal surface (TPMS) bone scaffold with multi-functional pores: lower stress shielding and higher mass transport capacity", Frontiers in Bioengineering and Biotechnology, vol. 12, 2024, p. 1401899.

[22]. A. P. G. Castro, J. Santos, T. Pires, and P. R. Fernandes, "Micromechanical Behavior of TPMS Scaffolds for Bone Tissue Engineering", Macromolecular Materials and Engineering, vol. 305, no. 12, 2020, p. 2000487. doi: https://doi.org/10.1002/mame.202000487.

[23]. B. Ziaie, X. Velay, and W. Saleem, "Exploring the optimal mechanical properties of triply periodic minimal surface structures for biomedical applications: A Numerical analysis", Journal of the Mechanical Behavior of Biomedical Materials, vol. 160, 2024/12/01/ 2024, p. 106757. doi: https://doi.org/10.1016/j.jmbbm.2024.106757.

[24]. F. Teng, Y. Sun, S. Guo, B. Gao, and G. Yu, "Topological and Mechanical Properties of Different Lattice Structures Based on Additive Manufacturing", Micromachines, vol. 13, no. 7, 2022, p. 1017. [Online]. Available: https://www.mdpi.com/2072-666X/13/7/1017.

[25]. C. Wang, D. Xu, L. Lin, S. Li, W. Hou, Y. He, L. Sheng, C. Yi, X. Zhang, and H. Li, "Large-pore-size Ti6Al4V scaffolds with different pore structures for vascularized bone regeneration", Materials Science and Engineering: C, vol. 131, 2021, p. 112499.

[26]. H. Abdulhadi, "Designing New Generations of BCC Lattice Structures and Developing Scaling Laws to Predict Compressive Mechanical Characteristics and Geometrical Parameters", Wright State University, 2020. [Online]. Available: http://rave.ohiolink.edu/etdc/view?acc_num=wright1610335306482598

[27]. R. Verma, N. K. Singh, S. K. Rai, and S. Kumta, "Triply periodic minimal surface porous implants to reconstruct bone defects", in Smart Healthcare for Disease Diagnosis and Prevention: Elsevier, 2020, pp. 21-28.

[28]. U. Simsek, A. Akbulut, C. E. Gayir, C. Basaran, and P. Sendur, "Modal characterization of additively manufactured TPMS structures: comparison between different modeling methods", The International Journal of Advanced Manufacturing Technology, vol. 115, 2021, pp. 657-674.

[29]. M.-T. Hsieh and L. Valdevit, "Update (2.0) to MiniSurf—A minimal surface generator for finite element modeling and additive manufacturing", Software Impacts, vol. 6, 2020, p. 100035.

[30]. N. S. Mustafa, N. H. Akhmal, I. Sudin, N. M. Yusof, and A. Idris, "Structural modulus of the unit cell of the bone tissue engineering scaffold based on Triply Periodic Minimal Surfaces (TPMS)", in AIP Conference Proceedings, 2024, vol. 2991, no. 1: AIP Publishing.

[31]. H. Zhang, S. Tang, H. Yue, K. Wu, Y. Zhu, C. Liu, B. Liang, and C. Li, "Comparison of computational fluid dynamic simulation of a stirred tank with polyhedral and tetrahedral meshes", Iranian Journal of Chemistry and Chemical Engineering, vol. 39, no. 4, 2020, pp. 311-319.

[32]. R. Noorossana, M. Shayganmanesh, F. Pazhuheian, and M. H. Rahimi, "Investigation of Laser Engraving Qualitative Characteristics of Al-SiC Composite Using Design of Experiments", Int. J. of Industrial Engineering & Production Research, vol. 31, no. 3, 2020, pp. 409-422.

[33]. N. Islahudin, D. S. Nugroho, Z. Arifin, H. Rahadian, and H. Suprijono, "Real-Time Scheduling Approach in Internet of

Things-Enabled Production Monitoring Systems", International Journal of Industrial Engineering, vol. 35, no. 4, 2024, pp. 1-17.

[34]. P. E. Seiler, K. Li, V. S. Deshpande, and N. A. Fleck, "The influence of strut waviness on the tensile response of lattice materials", Journal of Applied Mechanics, vol. 88, no. 3, 2021, p. 031011.

[35]. N. Kladovasilakis, K. Tsongas, I. Kostavelis, D. Tzovaras, and D. Tzetzis, "Effective Mechanical Properties of Additive Manufactured Strut-Lattice Structures: Experimental and Finite Element Study", Advanced Engineering Materials, vol. 24, no. 3, 2022, p. 2100879.

[36]. N. Sezer, Z. Evis, and M. Koc, "Additive manufacturing of biodegradable magnesium implants and scaffolds: Review of the recent advances and research trends", Journal of Magnesium and Alloys, vol. 9, no. 2, 2021, pp. 392-415.

Follow this article at the following site:

Nor Hasrul Akhmal Ngadiman, Nur Syahirah Mustafa, Izman Sudin, Denni Kurniawan. "Young's Modulus Optimisation of Triply Periodic Minimal Surfaces using Full Factorial Design" IJIEPR 2025; 36 (1): 171-180
URL: http://ijiepr.iust.ac.ir/article-1-2223-en.html